Int. J. Electrochem. Sci., 7 **(2012)** 3656 - 3671

International Journal of
ELECTROCHEMICAL
SCIENCE
www.electrochemsci.org

Groundbreaking Electrochemical Computation of Dispersed Individual Activation Energies and Development of Activation Energy Model for Chloride Induced Corrosion of RC Structures under Ambient Temperature

Raja Rizwan Hussain

Asst. Professor, CoE-CRT, Civil Engineering Department, College of Engineering, King Saud University, Riyadh, 11421, Saudi Arabia.
E-mail: raja386@hotmail.com

Received: 9 February 2012 / *Accepted:* 23 March 2012 / *Published:* 1 April 2012

In this paper a temperature dependent dispersed individual activation energy electrochemical approach is adopted which deals with chloride induced corrosion in reinforced concrete structures individually for every case of varying chloride concentration. Finally, an activation energy model is proposed based on the varying activation energies in relation to the coupled variation in chloride concentration and ambient temperature. Moreover, in this paper some interesting open ended queries, facts and findings related to the above area of research are also presented which open several significant future prospects of research in this direction. Reinforced concrete structures exposed to aggressive environments such as severe chloride attack coupled with high temperature suffer from accelerated corrosion. The objective of this paper is to model and verify the effect of temperature on chloride induced corrosion potential and corrosion rate of steel in concrete by incorporating novel approach towards computation of individual averaged activation energies based on Arrhenius plot. This paper presents a semi-empirical corrosion modeling approach which obeys the basic corrosion science laws and is also verified by the experimentation involving a wide range of chloride and temperature variations. The modeling task has been incorporated by the use of a concrete durability non-linear FEM model as a computational platform on which the coupled temperature-chloride induced corrosion throughout the life of reinforced concrete structures is examined in both space and time domains.

Keywords: temperature, chloride, sigmoidal growth equation, corrosion computation, activation energy model, reinforced concrete, electrochemistry

1. INTRODUCTION

In the previous research [1] the authors adopted an overall averaged approach for calculation of activation energy of the whole electro-chemical temperature induced corrosion modeling system. Here,

in this paper a more descriptive and innovative individual activation energy computational approach is introduced which deals with each case of chloride concentration individually one after the other. Finally, an activation energy model is proposed based of the varying activation energies in relation to the chloride concentration. Steel reinforcement corrosion in chloride contaminated concrete especially when coupled with high temperature is one of the major worldwide deterioration problems in reinforced concrete (RC) structures. Since chloride induced steel corrosion phenomenon is an electrochemical process, its rate is influenced by temperature. The high alkaline environment of good quality concrete forms a passive film on the surface of the embedded steel which normally prevents the steel from further corroding. However, under chloride attack, the passive film is destroyed, and the steel spontaneously corrodes. This phenomenon is much more accelerated when the climate is hot.

Many researchers have investigated the effect of temperature on chloride induced corrosion of RC structures [2-9]. The effect of temperature on corrosion is influenced by several factors and some of them have been overlooked in the past research works and have difference of opinion. Some researchers believe that corrosion rate is directly proportional to the increase in temperature while, others are of the opinion that the rate of increase in corrosion varies exponentially with the temperature rise. Yet some other researchers investigated that corrosion has very non linear or no specific relation with temperature and their experiment results showed a widely scattered trend. Details will be discussed in the following sections of this paper. It was found that the previous research data for the coupled effect of chloride and temperature on corrosion of reinforcement especially in the higher range is limited. Also, it was found that the numerical relation and experimental dependency of activation energy on the coupled effect of chloride and temperature needs to be further investigated. Therefore, it is necessary to conduct in-depth investigations in order to further understand the above said mechanisms. This leads to the objectives of this paper which is also a pending patent at the US patent office (File Number: 13304219/2011).

2. FEM COMPUTATIONAL APPROACH

The research methodology adopted in this paper is based on a 3D finite element model [1, 10-11]. It is a computational program for the evaluation of various durability aspects of concrete such as concrete hardening/hydration, microstructure formation and several associated phenomenon, from casting of concrete to a period of several months or years. As such this tool can be utilized to study the effect of ingredient materials, environmental conditions as well as the size and shape of structure on the durability of concrete. The term durability considered here takes into account both the fresh concrete problems as well as matured concrete exposed to environment. This tool can be used to analytically trace the evolution of microstructure, strength and temperature with time for any arbitrary initial and boundary conditions. Since the main simulation program is based upon finite-element methods, it could be applied to analyze real life concrete structures of any shape, size or configuration. Furthermore, dynamic coupling of several phenomenon ensures that the effect of changing environmental conditions is easily integrated into the overall simulation scheme.

A general frame work of mass and ion equilibrium equations and an electro-chemical reaction model of corrosion in reinforced concrete has been presented elsewhere [1, 10-11]. Thus the influential parameters on the theorem of corrosion process for the severe environmental effects are determined experimentally and simulated in numerical terms for the enhancement of existing model in this research.

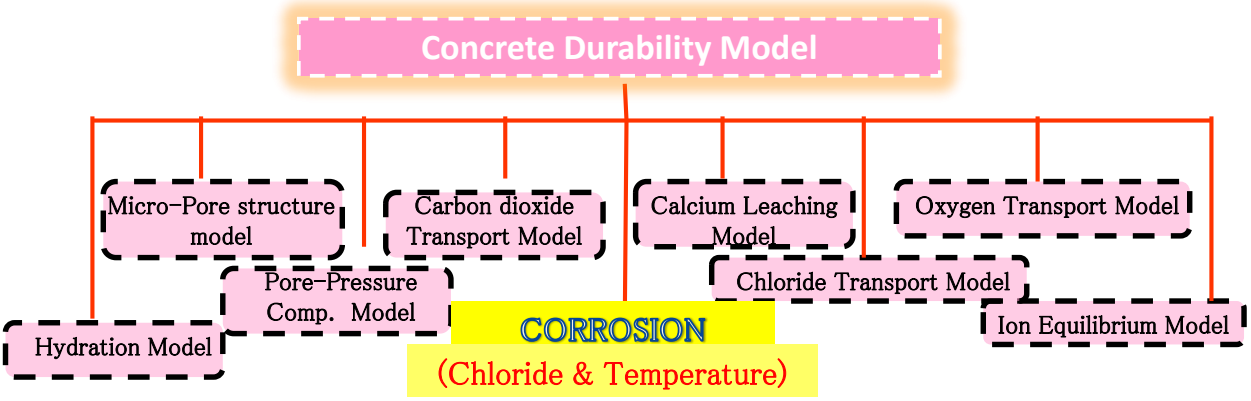

Figure 1. Unified Framework of Durability Concrete Model

The reliability of this model is verified through comparison of simulation with experiment results. The constituent material models employed as shown in Fig. 1 [10-11] are formulated based on micro-mechanical phenomena such as hydration, moisture transport and cementitious microstructure formation. Their strong interrelationships are taken into account by real time sharing of material characteristic variables across each sub-system. The non-linearity in corrosion process and the effect of severe environmental actions is taken into account automatically in the unified framework of this program by the help of various connected sub-models within this system to acquire the parameters necessary for computation of chloride induced corrosion of steel embedded in concrete under ambient temperature.

3. COMPUTATIONAL SIMULATION

The model is initially adopted from the previous research [1, 10-12]. In the model a general scheme of micro-cell corrosion is introduced based on electro-chemistry and classical Tafel diagram technique. The electric potential and current of corrosion cell is obtained from the ambient conditions which are calculated by other subroutines in the system.

3.1. Past Research: Comparison of Experiment Results and Model Analysis

The effect of temperature in previous corrosion model is considered from the original Nernst equations as temperature is one of the variables in these equations [10, 11]. The model does account

for the variation in temperature as far as the calculation of electrical potential is concerned. But, the model was primarily designed for constant normal temperature conditions for the calculation of electric current. Consequently, from the comparison of experiment results and model analysis, it can be seen that the model underestimates at high temperature conditions more than 20°C and required improvement as shown in Fig.2 and Fig. 3.

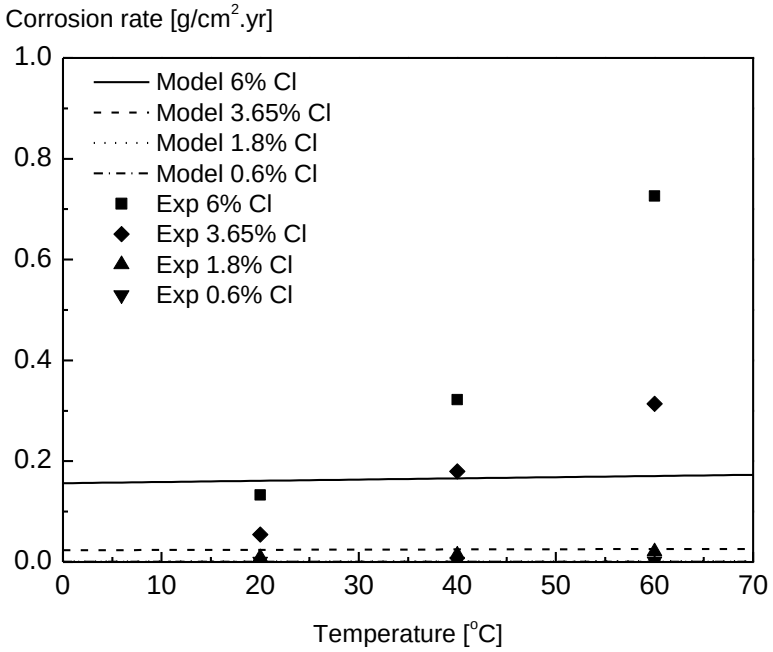

Figure 2. Temperature Vs corrosion rate profiles.

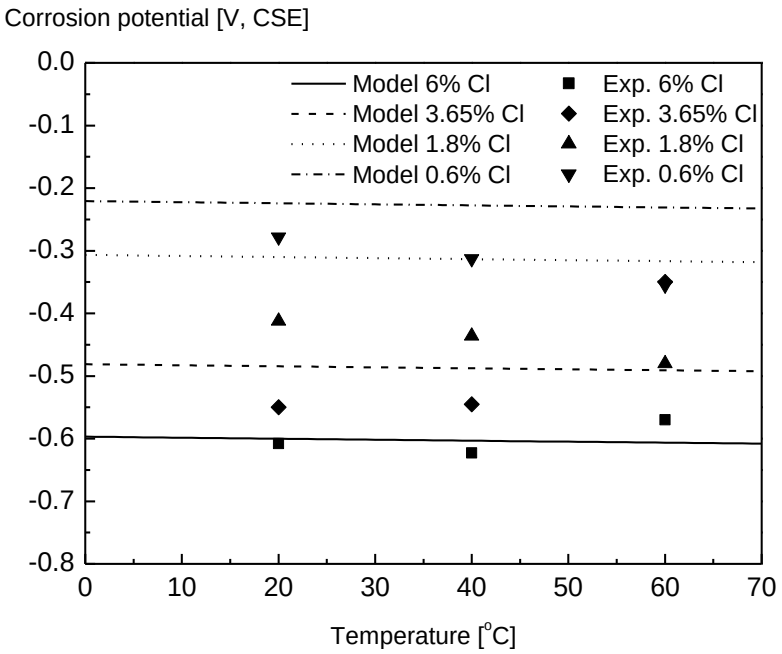

Figure 3. Temperature Vs corrosion potential profiles

3.2. Extension of chloride induced corrosion model for variable temperature conditions

It can be seen from the previous research that the model works satisfactorily for normal temperature conditions of 20°C (Figs. 2 and 3). In order to extend the model for variable temperature conditions in this paper, Tafel's equation derived from Arrhenius law has been modeled for the estimation of temperature induced corrosion in RC structures. The details of this extension are discussed as follows:

3.2.1. Corrosion in concrete and the effect of temperature

Since the corrosion of steel bars in concrete is an electrochemical process in nature, generally it is said that the electrochemical reaction is accelerated due to temperature. Therefore it is considered that the corrosion rate of a steel bar embedded in concrete rises up as the temperature rises. However, researches dealing with these matters were few [5]. Therefore, the objective of this research is to evaluate numerically and verify experimentally the temperature dependency of corrosion rates concerning steel bars embedded in concrete affected by chloride.

3.2.2 Theoretical discussion about dependency of corrosion reaction rate on temperature

In general, any chemical reaction rate is theoretically illustrated using Arrhenius Equation 1.

$$A = k \cdot \exp\left(-\Delta E_a / RT\right) \tag{1}$$

where, A: reaction rate, k: frequency factor, ΔE_a: activation energy, R: gas constant, T: Absolute temperature. The Equation (1) can be transformed into the logarithmic form as shown in Equation (2).

$$\ln A = -\left(\frac{\Delta E_a}{R}\right) \cdot \frac{1}{T} + \ln k \tag{2}$$

From Equation (2) it is apparent that the logarithm of the reaction rate ($\ln A$) is proportional to the reciprocal of the absolute temperature ($1/T$). And the diagram illustrating the relationship between the logarithm of the reaction rate and the reciprocal of the absolute temperature is called Arrhenius plot.

3.2.3. Electro-chemical temperature dependency of corrosion and limitations of the previous corrosion model

In the corrosion model under discussion, Nernst equations are used to calculate the respective half cell potential values on anode and cathode sites [11]. This is done to deal with the equilibrium

conditions concerning *E*, pH, concentrations of ions, partial pressures of gases, and so on, so that the model can predict the effect of various parameters related to corrosion of steel in concrete. No doubt these Nernst Equations are used in the model to understand the stable phase and reactions to be occurred in E-pH diagram, or Pourbaix diagram and Tafel's diagram [13]. But in the previous model, only respective potentials and slopes are calculated with respect to temperature. The Tafel slope b_a in the previous model increases with higher temperature and it causes reduction in the corrosion current i_{corr}. This is the reason for under estimation of temperature induced corrosion model.

At a later stage it was found that in the previous model [12] not only the slope b_a but also the exchange electric current density at anode i_o^a also increases with higher temperature and needs to be incorporated in the model. From the past research works [14, 15], it is found that the effect of temperature is much higher on i_o^a than on b_a. As a result, even though the slope b_a increases with temperature causing decrease in i_{corr}, the increase in i_o^a is much higher. This results in overall increase in the corrosion current. So far in the previous model, a standard constant value of i_o^a was used as 1.0×10^{-5}A/m^2. This value is satisfactorily enough when one uses a constant normal temperature model for 20°C. But when it is intended to extend the model for variable temperature conditions in this paper, then need is felt to install the effect of temperature from the original Arrhenius Law as shown in Equation 3 below.

$$i_{o\,(T)}^a = (i_o^a)_\infty \exp(-\Delta E_a/RT) \qquad (3)$$

where;

$i_{o\,(T)}^a$:anodic current at temperature '*T*'

$(i_o^a)_\infty$:ultimate reference anodic current at infinite temperature (an imaginary situation)

3.2.4. Method adopted for back calculation of parameters, assumptions and verification for applicability of Arrhenius Law by Arrhenius plot analysis

It is not easy to get the value of 'i_o^a' directly from experiment results only. Therefore, it was decided to back calculate the values of 'i_o^a' at 20, 40 and 60°C by the sensitivity analysis in comparison to the experiment data and drawing of the Arrhenius plot for checking the applicability of Arrhenius Law and the determination of activation energy.

3.2.4.1 Assumptions and limitations

In the back calculation of anodic current 'i_o^a' from the corrosion current '$i_{corr.}$' it is assumed that the corrosion reaction follows a reversible path under ideal conditions, the law of mass-energy conservation is applicable, the corrosion product is assumed to be uniform over the entire surface area of rebar and formation of pits due to localized attack is not treated separately but given an average treatment. Considering the air dry conditions for free flow of oxygen, it is assumed that the variation in

the solubility of oxygen in water due to variation in temperature will not effect significantly on the cathodic slope 'b_c'. Thus, same value of cathodic slope has been used as in the constant temperature model earlier. The effect of concentration polarization and other non-equilibrium processes remain for future research. Overall, a simplified and practical methodology is adopted.

3.2.4.2 Setting of referential value at 20°C

The referential temperature has been set at 20°C and the standard value of $i_o^a = 1.0\text{x}10^{-5}\text{A/m}^2$ which was used as a constant value of anodic current in the original model has been set as the referential value of anodic current at 20°C in the enhanced model in this paper. With reference to the previous literature review [16], the Equation 4 can be narrated as follows for the setting of referential values.

$$i_{o\,(T)}^a = i_{o\,(Ts)}^a \exp\left[-\Delta E_a/R\,(1/T - 1/T_s)\right] \quad (4)$$

where;

$i_{o\,(Ts)}^a = i_{o\,(\infty)}^a \exp[-\Delta E_a/R(1/T_s)]$

Here in Equation 4 the value of referential anodic current '$i_{o\,(Ts)}^a$' is equal to $i_{o\,20^oC}^a = 1.0\text{x}10^{-5}$ A/m^2. This enhanced model derived from Arrhenius law gives the direct relation between the anodic current 'i_o^a' and any arbitrary temperature *T*.

3.2.4.3 Back calculation procedure for finding 'i_o^a' values for variable temperature conditions of 40°C and 60°C

As there is no way to measure the value of 'i_o^a' directly from experimentation, therefore, the referential values of 'i_o^a' at 40 and 60°C are back calculated by using standard referential value of $i_o^a = 1.0\text{x}10^{-5}\text{A/m}^2$ at 20°C along with sensitivity analysis on the corrosion model. Originally the back calculation is done starting from the corrosion current and potential. Corrosion potential is obtained as direct measurement while corrosion current is obtained from the gravimetric mass loss measurement in the experiment by using Faraday's law. Then using Nernst Equation in the model and comparison of experiment results and analysis (Fig. 2 and Fig. 3), the respective values of anodic current 'i_o^a' at 40 and 60°C are back calculated by performing sensitivity analysis, so that the model analysis and experiment results become coherent on averaged basis for all the available cases of variable chloride and temperature conditions.

3.2.4.4 Applicability of Arrhenius Law and authenticity of the above procedure

The anodic current values 'i_o^a' obtained as above were plotted against the inverse of absolute temperature to obtain what is called Arrhenius plot. It was observed that the Arrhenius plot came out to

be a straight line (Figure 4). Thus proving the fact that Arrhenius Law is applicable and the proposed enhancement method is valid.

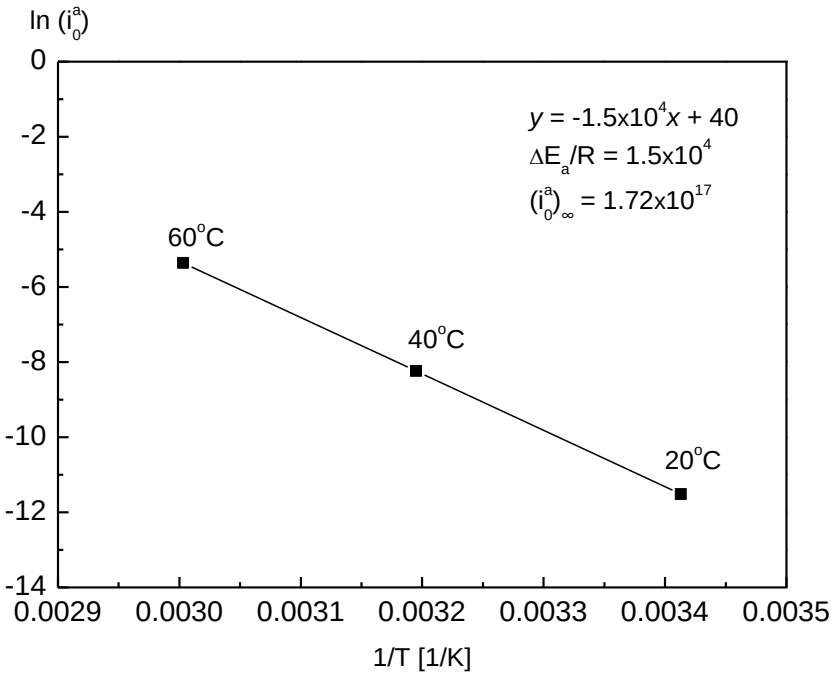

Figure 4. Arrhenius plot for referential anodic current 'i_o^a' values at 20°C, 40°C and 60°C.

3.2.4.5 Calculation of Individual Dispersed Activation Energies

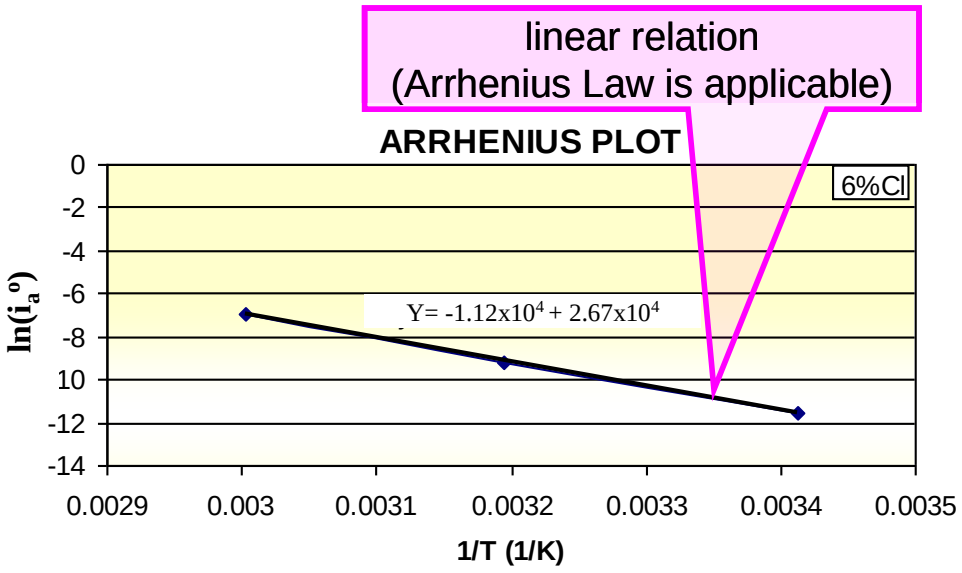

Figure 5. Arrhenius plot for 6% total Cl experiment data at 20, 40 and 60°C.

By the methodology discussed in the previous section the anodic current values 'i_o^a' were obtained for one extreme case of chloride concentration i.e; 6% total chloride by mass of binder and plotted against the inverse of absolute temperature to obtain the Arrhenius plot for one individual case. It was observed that the Arrhenius plot again came out to be a perfect straight line (Fig. 5) even for an individual case. Thus proving the fact again that Arrhenius Law is applicable and the newly invented individual dispersed activation energy enhancement method is valid. `As it is evident from Figure 5 that the rate of increase of 'i_o^a' with temperature follows Arrhenius Law, activation energy can now be obtained for this individual case as well. From this Arrhenius plot, activation energy of reaction came out to be '$\Delta E_a = 1.12 \times 10^4 \times R$' and the referential value '$(i_o^a)_\infty$' which is the ultimate reference anodic current at infinite temperature is calculated as '$(i_o^a)_\infty = 4.04 \times 10^{11}$'.

3.2.4.6 Comparison of enhanced temperature model with experiment results

The corrosion model shows good agreement with the experiment results (Fig. 6) for the effect of temperature on corrosion of steel reinforcement embedded in concrete for 6% chloride concentration. Thus, providing evidence for the efficiency and accuracy of the proposed individual dispersed modeling computational approach. The Fig. 7 explains the overall picture of above methodology adopted in this research. It explains the applicability of Arrhenius law and authenticity of the proposed procedure, the results of Arrhenius plot and the linear relation obtained, calculation of activation energy, its application for the prediction of temperature induced corrosion in RC structures and finally the comparison of experiment results and analysis which shows a good match.

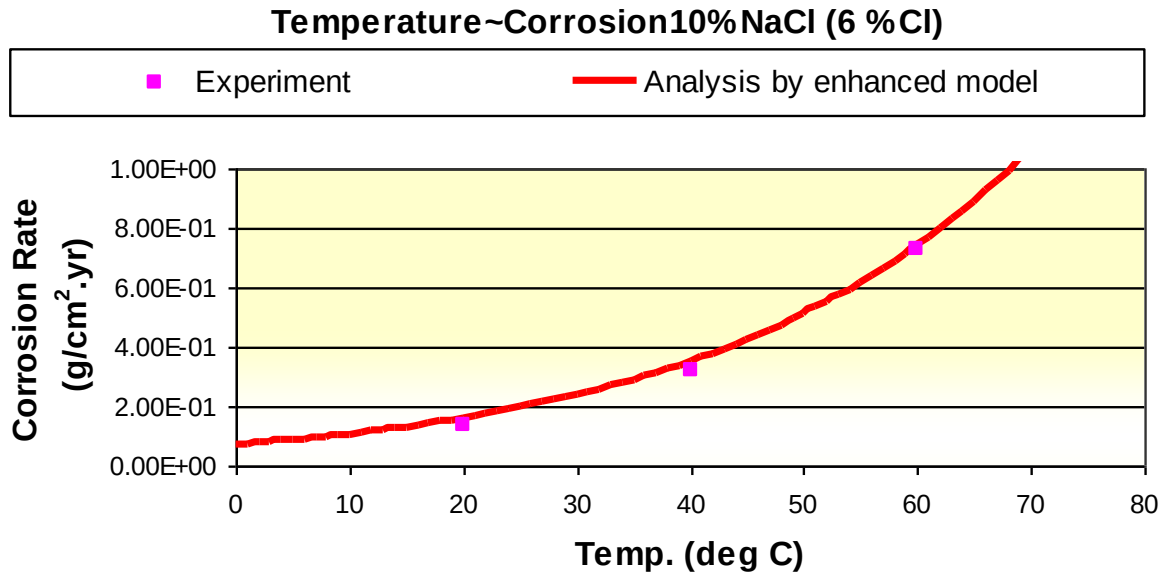

Figure 6. Temperature Vs corrosion rate profile (6% Cl)

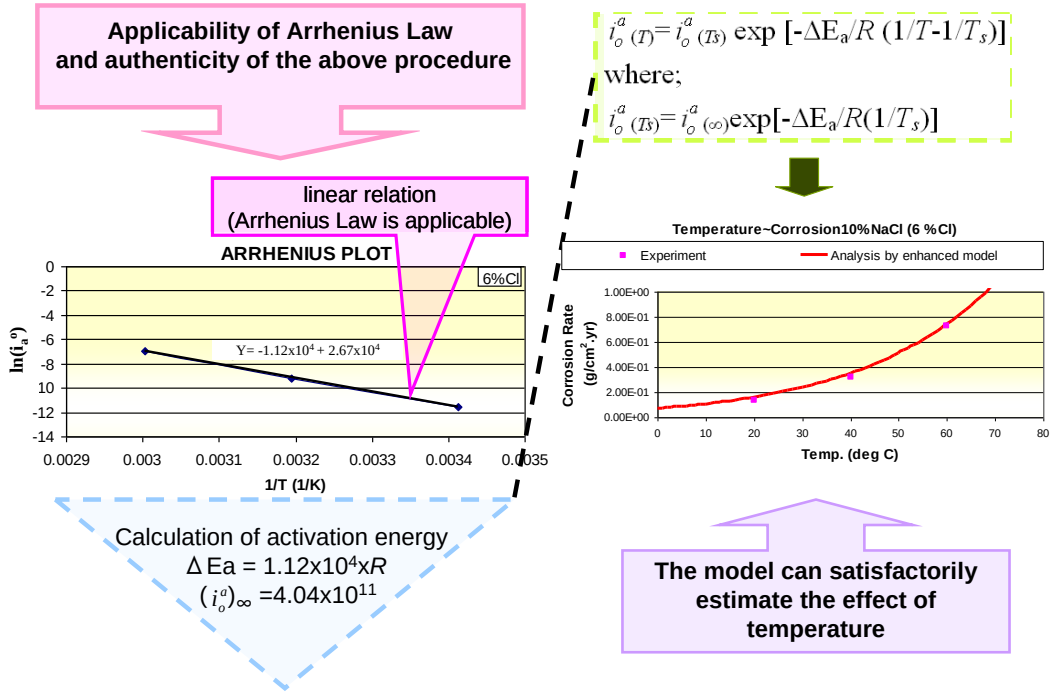

Figure 7. Modeling of temperature at variable temperature conditions and setting of referential values

3.2.5 Extension of enhanced temperature induced corrosion model for variable chloride concentration cases and successive verification

In order to apply the enhanced temperature model to varying percentage of chloride concentrations, Arrhenius plots are made on similar lines as explained above in previous sections for various cases of chloride concentrations and analyzed individually as well as in comparison to each other.

3.2.5.1 Detailed analysis of Arrhenius plots for various chloride cases

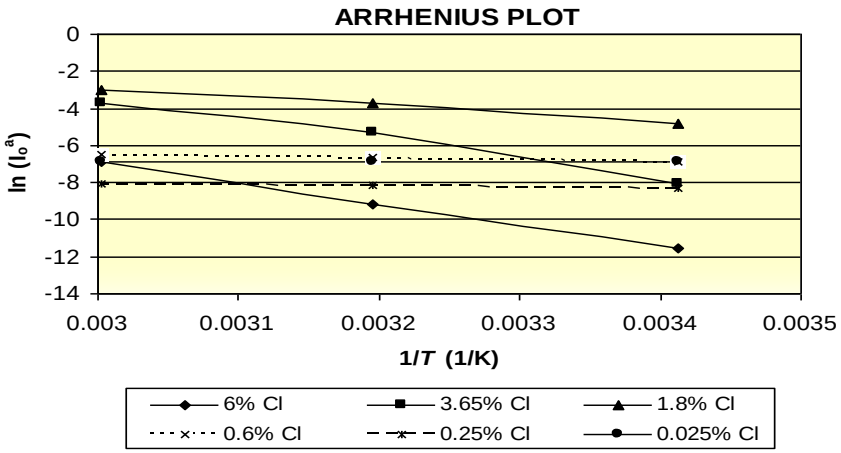

Figure 8. Arrhenius plot for variable total chloride dispersed experiment data at 20, 40 and 60°C.

It can be seen that all the chloride cases show linear Arrhenius plots (Fig. 8) and for these Arrhenius plots, model analysis and experiment results [1, 12] show a perfect match (Fig. 9 and Fig. 10).

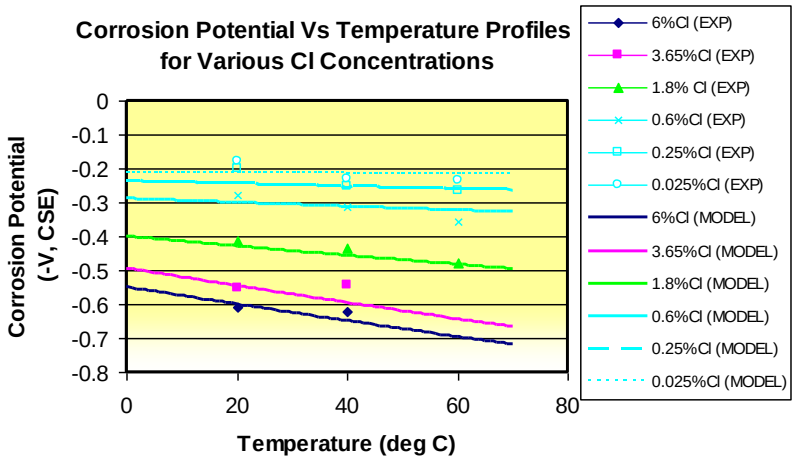

Figure 9. Comparison of enhanced temperature model for the estimation of corrosion potential under variable chloride environment

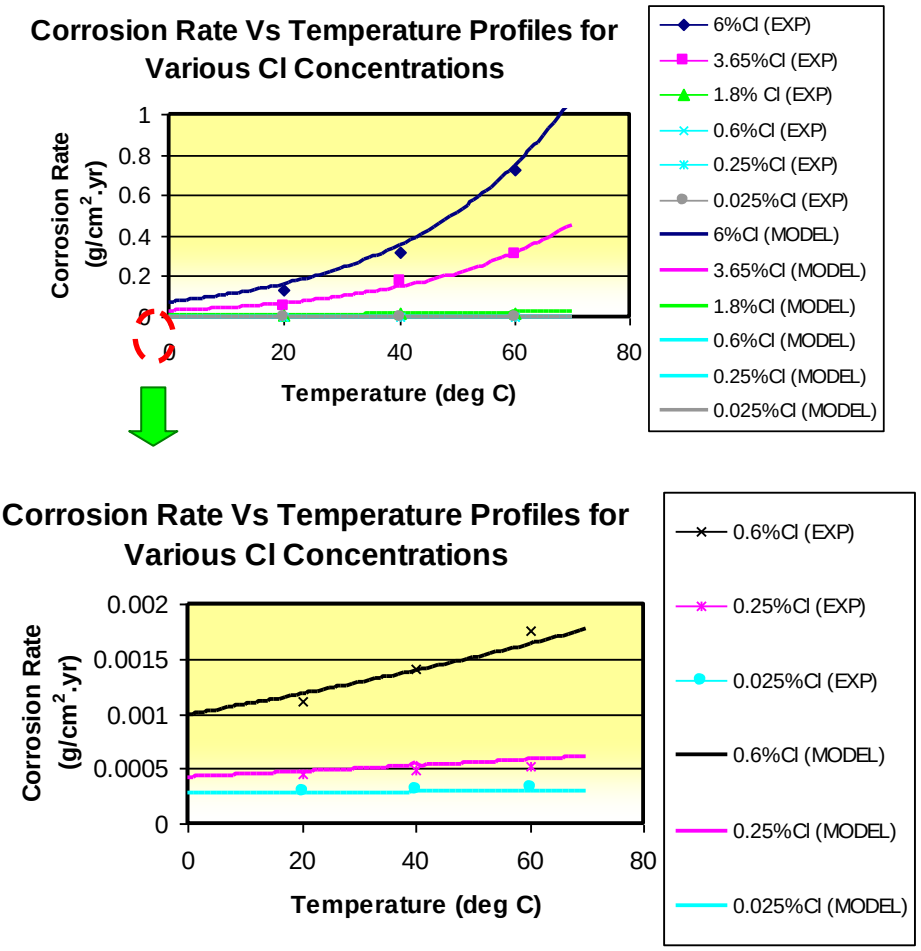

Figure 10. Comparison of temperature model for the estimation of corrosion rate under variable chloride environment

Thus proving the fact again that Arrhenius Law is applicable and the proposed enhancement method is valid for various individual and dispersed chloride concentration cases. But, comparing the Arrhenius plots with each other it can be seen that the activation energies are different for different cases of chloride concentrations.

3.2.5.2 Behavior and dependency of activation energy

To understand the behavior of activation energy in chloride induced corrosion reaction, activation energy profile as a function of chloride content is extracted from Fig. 8 and presented as Fig. 11 to understand the non-linear individual dispersed activation energy behavior.

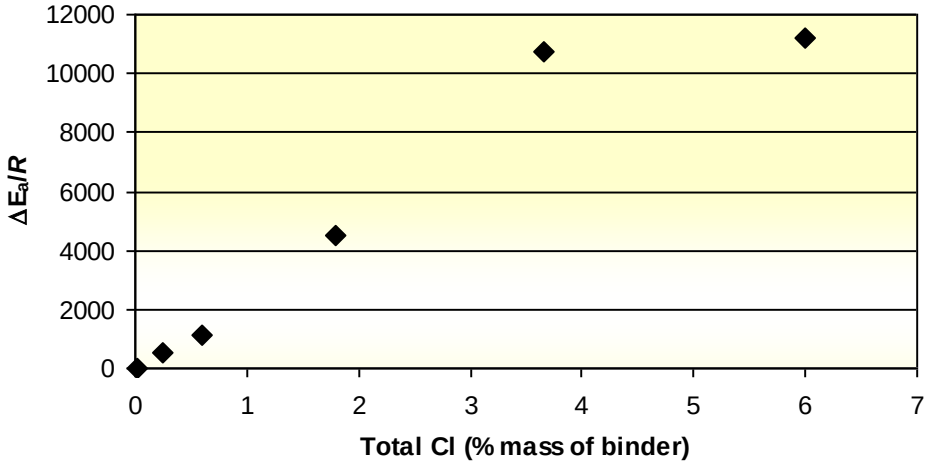

Figure 11. Relation of activation energy with chloride concentration in corrosion reaction

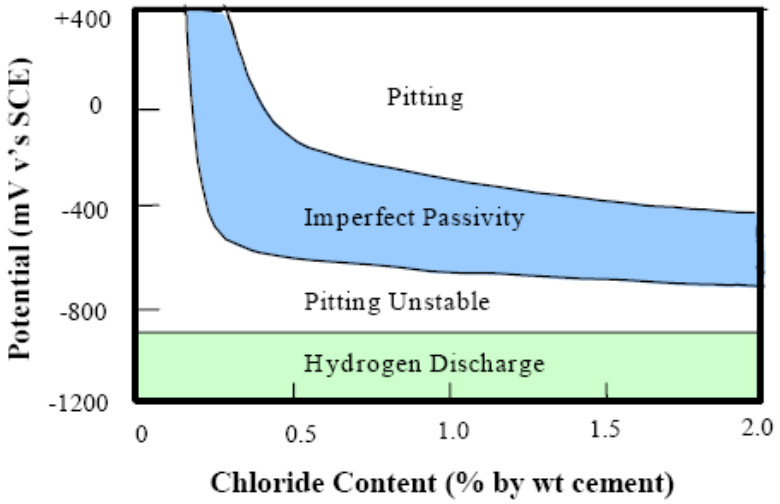

Figure 12. Approximate domains of electrochemical behavior of steel in concretes with different levels of chloride contamination.

From this profile it can be seen that activation energy is directly proportional to the increase in chloride concentration. The reason lies in the nature of the effect of chloride on corrosion reaction. Principally the activation energy is independent of the amount of reactants and products. But, in fact chloride is not the main reactant or product of corrosion reaction and the function of chloride is to make the initiation only by indirect reaction with the passive layer.

The exact methodology and equilibrium equations involved in the attack of chloride on the passive layer is still unknown to the researchers and inherits a difference of opinion. From the previous research (Fig. 12) [17-19], it can be seen that the electrochemical behavior of steel bar varies with concentration of chloride in concrete. Thus different levels of chloride concentration can change the nature of corrosion reaction. In other words, the type of reactants and products involved in corrosion reaction change with varying concentration of chlorides in concrete. Thus ultimately different amounts of chloride concentration result in different amounts of activation energies in corrosion reaction of steel in concrete.

3.3 Modeling trends of activation energy and chloride profile

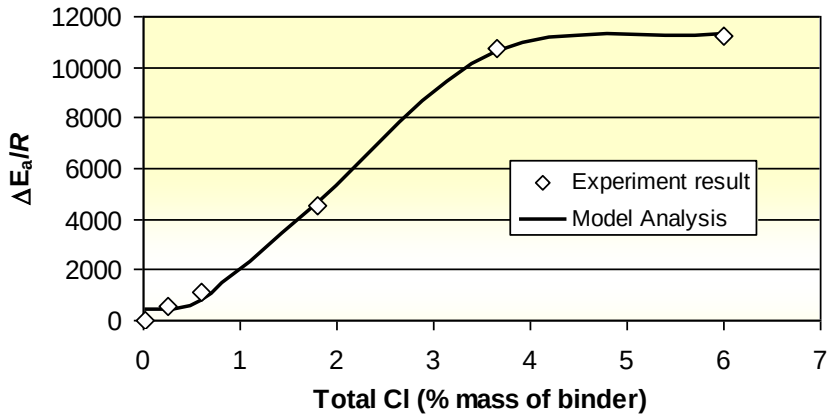

Figure 13. Comparison of Sigmoidal equation and experiment results

The relation between activation energy and chloride content in corrosion reaction is analyzed on theoretical grounds and it is revealed that it follows the sigmoidal growth equation 5.

$$Y = A - (A-B)e^{-(kX)d} \quad (5)$$

Where;

$Y = \Delta E_a/R$; X= Total Cl (% mass of binder); A, B, k and d are constants; A= 11294; B= 400; k= 0.42

d= 2.45. The comparison of analysis by Eq. 5 and experiment results [1, 12] shows good agreement as shown in Fig. 13.

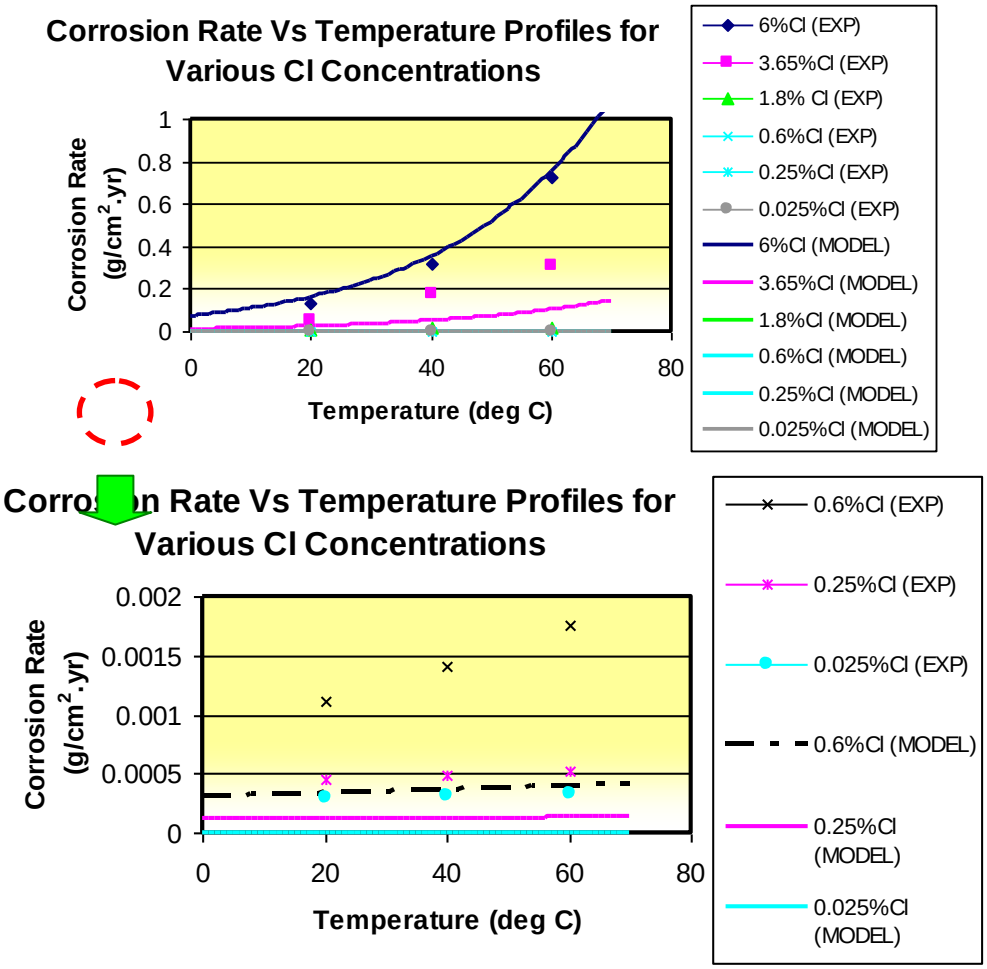

Figure 14. Comparison of temperature model for the estimation of corrosion rate under variable activation energy and chloride

Using the above model and the standard value of $i_o^a = 1.0\text{x}10^{-5}\text{A/m}^2$ as the referential value of anodic current at 20°C , which was used as a constant value of anodic current in the original model, the experiment results and model analysis is compared for corrosion current and potential values in Fig. 14 and Fig. 15.

It can be seen that except the case of 6% total chloride content, all other cases do not show good agreement between the experiment results and model analysis. This is because the standard value of $i_o^a = 1.0\text{x}10^{-5}\text{A/m}^2$ at 20°C match with the i_o^a of 6% chloride case but is different for other cases of chloride concentration and temperature conditions (Fig. 8). When same value of i_o^a is used for all cases of chloride concentration then the situation shown in Fig. 16 is obtained. The averaged arrhenius plots for linear and non linear values do not overlap each other and create a difference. When all the Arrhenius plots are converged at a single point, the curves do not remain parallel and linear any more. This remains as a scope for future research.

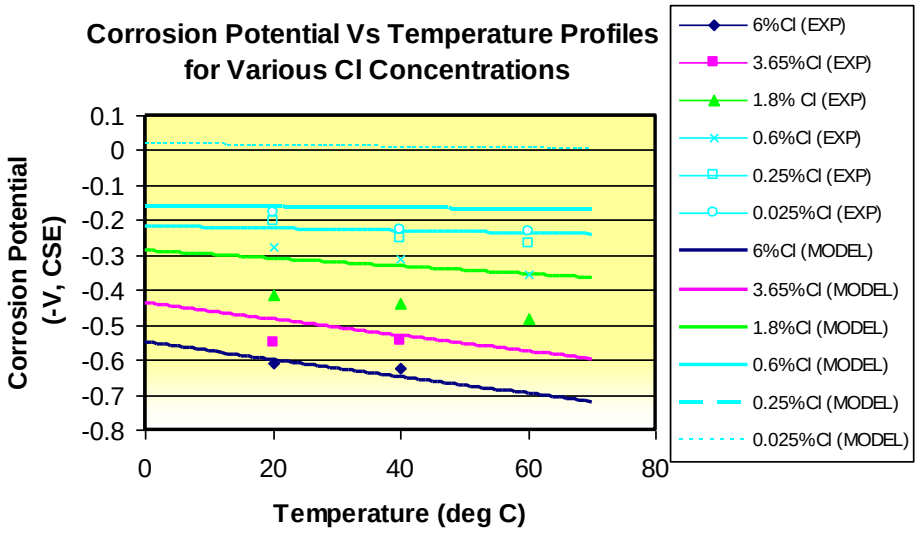

Figure 15. Comparison of temperature model for the estimation of corrosion potential under variable activation energy and chloride

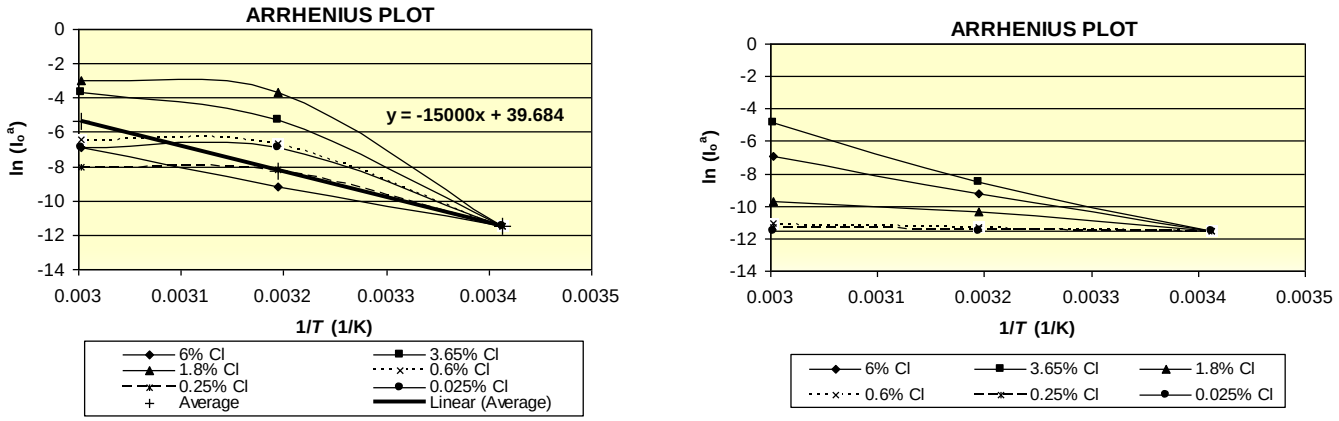

Figure. 16 Arrhenius plot for variable activation energy and standard i_o^a referential value at 20°C.

4. CONCLUSIONS

The approach presented in this paper is unique, advanced and more accurate than the one presented in the past research since it takes into account the dispersed activation energy model concept instead of integrated averaged activation energy approach presented in the previous research [1]. The model based on the novel approach towards modeling of dispersed individual activation energy from the Arrhenius plot developed in this paper being in close agreement with the experiment results predicts the corrosion rate and potential for the coupled effect of a wide range of temperature and chloride conditions with good accuracy and precision. Tafel's equation derived from Arrhenius Law has been semi-empirically modeled for the estimation of the effect of temperature on chloride induced corrosion in RC structures. Thus the effect of temperature corrosion obeys the Arrhenius equation.

Influential semi-empirical parameters for modeling and prediction of the effect of temperature on chloride induced corrosion of steel in concrete are experimentally determined and numerically discussed through electrochemical formulations.

ACKNOWLEDGEMENT
The author gratefully acknowledges the support by King Saud University, Deanship of Scientific Research, College of Engineering Research Center.

References

1. Hussain Raja Rizwan and Tetsuya Ishida, *Journal of ASTM International*, 7 (2010), DOI: 10.1520/JAI102667.
2. M. Wasim and Hussain Raja Rizwan, *Int. J. Electrochem. Sci.*, 7 (2012)1412-1423.
3. Maruya, T., Kailin Hsu, Hitoshi Takeda and Somnuk Tangtermsirikul, *Journal of Advanced Concrete Technology*, 1 (2003) 147.
4. T. Maruya, H. Takeda, K. Horiguchi, S. Koyama and K.-L. Hsu, *Journal of Advanced Concrete Technology*, 5(2007) 343-362.
5. Takahiro Nishida), *Thesis PhD, Tokyo Institute of Technology*, Japan, (2005).
6. Byung Hwan Oh, Bong Seok Jang and Seong Cheol Lee, *Proceedings of the 11th international workshop on Microstructure and Durability*, Sapporo, Japan (2004).
7. Hussain Raja Rizwan, *Int. J. Electrochem. Sci.*, 7 (2012) 1402-1411.
8. V. Zivica, *Indian Academy of Sciences, Bull. Mater. Sci.*, 25 (2002) 375.
9. P. Lambert and C.L. Page, *Materials and Structures*, 24 (1991) 351.
10. Ishida, T., and Maekawa, K., *Journal of JSCE*, 44(1999) 627.
11. Koichi Maekawa, Tetsuya Ishida and Toshiharu Kishi, *Journal of Advanced Concrete Technology*, 1 (2003) 91-126.
12. Hussain Raja Rizwan and Tetsuya Ishida, *Construction and Building Materials Journal*, 25 (2011) 1305-1315.
13. Denny, A.J., *New Jersey, Prentice Hall* (1996).
14. D.Piron, *NACE International* (1991).
15. Vaccaro, F.J., Rhoades, J., Le, B., *Telecommunications Energy Conference*. 19(1997) 230-237.
16. K. Maekawa, R. Chaube and T. Kishi, *Modelling of Concrete Performance, E & FN SPON*, (1999).
17. G. Sergi and C.L Page, *The European Federation of Corrosion*, 31(2000) 93.
18. L. Bertolini, F. Bolzoni, A. Cigada, T. Pastore, & P. Pedeferri, *Corrosion Science*., 35 (1993) 1633-1639.
19. Luca Bertolini, Bernhard Elsener, Pietro Pedeferri and Rob Polder, *Wiley-Vch Verlag* GmbH and Co. kGaA (2003).